MALAYSIAN JOURNAL OF SCIENCE
MJS
ISSN 1394-3065

Regular Issue

Malaysian Journal of Science 42 (3): 45-55 (Oct 2023) https://mjs.um.edu.my

SYNTHESIS, PHYSICOCHEMICAL ELUCIDATION AND BIOLOGICAL SCREENING STUDY OF NEW LIGAND DERIVED FROM 5,6-O-ISO PROPYLIDENE-L-ASCORBIC ACID AND ITS METAL(II) COMPLEXES

Fawzi Yahya Wadday[1a], Lekaa Khalid Abdul Karem[2b], Duha Mohammed Mortatha[3c]

Abstract: A simple chemistry method approach was used to synthesise new ligand derivate from L-ascorbic acid and its complexes. All of them were water-soluble and are used quite extensively in the medical and pharmaceutical fields. This study synthesised the new ligand derivative from L-ascorbic acid-base using the following steps: A 5,6-O-isopropylidene-L-ascorbic acid was prepared by reacting dry acetone with L-ascorbic acid followed by reacting it with trichloroacetic acid to yield [chloro(carboxylic)methylidene]-5,6-O-isopropylidene-L-ascorbic acid in the second stage. In the third stage, the derivative was reacted with (methyl(6-methyl-2-pyridylmethyl)amine to create a new ligand (ONMILA). This novel ligand was identified using a number of techniques, namely mass spectroscopy, 1H, 13C-Nuclear magnetic resonance, Fourier Transform Infrared (FT-IR), and Ultraviolet–visible (UV-Vis) spectra. It was observed that several complexes formed between the ligand and divalent metal ions (Co, Ni, Cu, Zn, Cd). Based on Micro Elemental Analysis, the mole ratio was (1:1) (M:L). Magnetic susceptibility, elemental analysis (C.H.N.O) procedures, molar conductivity tests, and proportion of metal ions calculations were used to describe the complexes. The findings showed the novel ligand had a mono, negative charge and behaved like a tridentate ligand type (N.N.O.). Therefore, the octahedral formula is suggested for all compounds. Only one spot was observed on thin layer chromatography (T.L.C.) for ligand (L) and complexes, indicating that the reaction completed and delivered only a single product. These chemicals have been connected to both Gram-negative and Gram-positive bacteria. The results suggested that antibacterial activity in metal complexes is higher than in the free ligand.

Keywords: *L-ascorbic acid, ligand, techniques, metal complexes, antibacterial activity*

1. Introduction

L-enantiomer of ascorbic acid without scurvy is a condition caused by vitamin C deficiency (Zümreoglu-Karan, 2006). The human body requires a robust immune system and therefore, a vitamin-rich daily diet is recommended. Vitamins with critical biological properties are abundant in natural foods, particularly vegetables and fruits, which are rich in cinnamon, vitamin C, and hesperidin and well-known for their health benefits (Bellavite & Donzelli 2020). L-ascorbic acid is a type of vitamin C which has water-soluble antioxidants and a protective function. Although most mammals can produce ascorbate, they cannot produce vitamin C (Chatterjee, 1973). L-ascorbic acid is a biological antioxidant (Loke et al., 2006) that protects the cell from damaging radicals, especially those generated during incomplete O2 oxidation (Padayatty et al., 2003). In both chemistry and biology, L-ascorbic acid is a critical chemical and its complexes are significant in both (Hanukoglu, 2006). Although ascorbic acid has many antimicrobial effects, some of its oxidative products are toxic (Hollis et al., 1985). According to Fodor (1983), L-ascorbic acid molecule has four hydroxyl groups which participate in conventional esterification. It is possible to use L-ascorbic acid (L-asc.) or Vitamin C and its derivatives in various biological and industrial uses (John & James, 2009). It has several donors, atoms, O(1), O(2), O(3), O(5), and O(6), that are usually involved in metal-ligand bonding (Tajmir-Riahi, 1990). The functional groups -OH,-COOH,-SH,-NH2 in derivatives of L-asc. have been found to coordinate with metal ions and form complexes [10]. These vitamin-metal complexes are essential in development of medication and nutrition (Wasi, 1987) while metal complexes are crucial for the pharmaceutical and agricultural industries. A living system relies heavily on trace amounts of metal elements and these transition metal ions ensure that different enzymes function correctly (Hariprasath et al., 2010). The current study examined these metal complexes for their antiseptic action alongside various bacterial strains. Their antibacterial activity was found to be effective against all the strains The study also attempted to establish and validate a new apparent synthesis and description of an L-ascorbic acid derivative ligand (L).

Authors information:
[a]Kufa University, Faculty of Science, Chemistry Department, Najaf, IRAQ. E-mail: fawzi.almuwashi@uokufa.edu.iq[1]
[b]Baghdad University, College of Education for Pure Sciences, Ibn/Al-Haitham Chemistry Department, IRAQ. E-mail: likaa.k.a@ihcoedu.uobaghdad.edu.iq[2]
[c]Kufa University, Faculty of Pharmacy, Department of Pharmaceutical and Industrial Pharmacy, Najaf-IRAQ. E-mail: duham.najaf@uokufa.edu.iq[3]
*Corresponding Author: fawzi.almuwashi@uokufa.edu.iq

Received: September 27, 2022
Accepted: December 24, 2022
Published: October 31, 2023

DOI:https//doi.org/10.22452/mjs.vol42no3.7
Malaysian Journal of Science 42(3): 45-55 (October 2023)

2. Experimental

2.1 Instrumentation

Shimadzu FT-IR spectrophotometer ranging 4000-400 cm^{-1}, Shimadzu UV-Vis. spectrophotometer with 200-1100 nm", Stuart electrothermal equipment, model SMP30 W.T.W. in OLAP cond 720 digital conductivity meter, Bruker D.R.X. (500-MHz, DMSO-d_6) spectrometer, mass spectrometer 5975 quadrupole. Elemental analyser Euro Vectro-3000A, Atomic absorption spectrophotometer Analytic Jena (A.A350), Magnetic Susceptibility Balance Mode (MSB-MKI). 854 Schwach Autoclave, Gallen Kamp Sterilizer, Memmert Incubator.

2.2 Materials

L-ascorbic acid, Trichloro acetic acid, Potassium hydroxide, Methyl(6-methyl-2-pyridylmethyl) amine, Metal chloride "$CoCl_2.6H_2O$, $NiCl_2.6H_2O$, $CuCl_2.2H_2O$, $ZnCl_2$, $CdCl_2.H_2O$", Mueller Hinton agar, dry acetone, N-Hexane, Dimethylsulfoxide, Dimethylformamide, HCl gas, Ethanol, Distilled water. "All chemicals used were of the highest purity. B.D.H., Fluka, and Merck were used without further purification.

2.3 Synthesis of The New Ligand (L)

2.3.1 Synthesis of 5,6-O-iso propylidene-l-ascorbic acid:

A 250 mL flask containing 0.528 grams (0.003 moles) of L-ascorbic acid powder along with 50 mL of dry distillers acetone was given a rapid bubble bath of dry hydrogen chloride and stirred for 20 minutes. The supernate was decanted after 20 mL of n-hexane was added followed by additional stirring and then chilling (ice-water). After each addition, the precipitate was rinsed with (100 mL) of the acetone-hexane combination (3:7) (v/v) followed by stirring, cooling in cold water, and then extracting the supernate. This process was repeated four times. The final precipitate was subjected to drying under decreased pressure, which resulted in the production of a white crystalline residue with a melting temperature of 216 °C. This yielded 70.51 grams R_f (0.69) in benzene:ethanol (8:2) (v/v) solvent solution.

2.3.2 Synthesis of [Chloro(Carboxylic)Methylidene)]-5,6-Isopropylidene-L-Ascorbic Acid:

5,6-O-isopropylidene-L-ascorbic acid (0.432 g, 0.002 mole) was dissolved in (25 mL) ethanol. A potassium hydroxide solution (0.112 g, 0.002 moles) in ethanol (20 mL) was later added and stirred for 30 minutes. Next, trichloro acetic acid (0.163 g, 0.001 mole) in ethanol (15 mL) solution was added and left for one hour. The product was filtered. Recrystallisation from 25mL (20 mL ethanol + 5 mL water) yielded 73.5% of pale brown solid crystalline residue with a melting point of 209 °C. (benzene: methanol) R_f 0.57 in (5:5).

2.3.3 Synthesis of The Ligand (L), [O, O-2,3-(N-Carboxylicmethylidene)-N-Methyl-1-(6-Methylpyridyl]-5,6-Isopropylidene-L-Ascorbic Acid:

0.306 g (1 mmole) of methylidene-(chloro(carboxylic)-5,6-iso propylidene-L-ascorbic acid was diluted in 20 mL ethanol. Using methyl (6-methyl-2-pyridylmethyl)amine, the solution was dropped wide (0.14 mL, 0.001 mole) and refluxed for two hours. A deep dark precipitate mass formed after some time at room temperature, and which was subsequently separated from the solution. Recrystallising the resulting mass in ethanol yielded a brown crystalline substance with a melting point of (127 °C) and a yield of 80.47 percent. R_f (0.48) in a solvent solution of benzene and ethanol (8:2) (v/v). The diagram below (Scheme 1) describes the reaction.

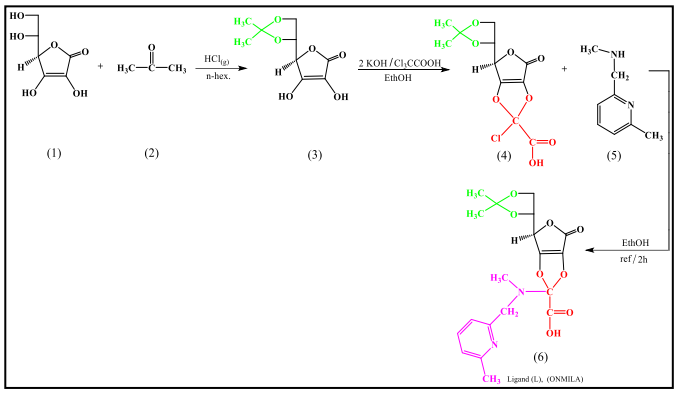

Scheme 1. Synthesis route of a new ligand (ONMILA) derivative.

2.3.4 Synthesis of Metal Complexes

1 mmol metal chloride 0.238 g $CoCl_2.6H_2O$, 0.237 g $NiCl_2.6H_2O$, 0.170 g $CuCl_2.2H_2O$, 0.136 g $ZnCl_2$, 0.183 g $CdCl_2.H_2O$ in 10 mL ethanol solution was added to a mixture of ligand (0.406 g, 1 mmol) in 10 mL ethanol. After agitating the solutions for an hour, the complexes were gently precipitated by evaporation. Figure 9 describes the process of recrystallising the complexes from heated ethanol. Water, methanol, ethanol dimethylsulfoxide, and dimethylformamide are all effective for dissolving isolated complexes which are colourful solids that are stable in air but insoluble in normal organic solvents. Table 1 describes the physical characteristics and provides analytical data for ONMILA and its complexes.

2.4 Biological Activity

The agar-well diffusion technique was applied in the testing of synthesised ligand and complexes against Staphylococcus aureus and Streptococcus pyogenes which are Gram (+), E-coli and Klebsiella pneumonia, Gram (-). All of the compounds were found to be effective against the bacteria (Al-Khafagy, 2016; Valarmathy et al., 2020). Muller Hinton Agar was used as the medium for the cultivation of the microorganisms to be tested. Dimethyl sulfoxide (DMSO), was used as a solvent in a single concentration of $1x10^{-3}$ M to make the chemical solutions; this was aimed at studying its biological activity. The plates were kept in an incubator at 37 °C for a whole day. The compounds' antibacterial activity was evaluated with regard to the size of the inhibition zone they produced against the particular strain of bacteria tested. The growth inhibition zone for each sample was determined by utilising the mean value obtained from three separate repetitions in order to reach a conclusion.

DOI:https//doi.org/10.22452/mjs.vol42no3.7
Malaysian Journal of Science 42(3): 45-55 (October 2023)

3. Results and Discussion

3.1 Physical Characteristics and Elemental Examination

Table 1 shows physical features and results of elemental analysis (C.H.N.O) examination and the organized compounds' metal substances.

Table 1. Physical properties and analytical statistics of ONMILA and its complexes

Empirical formula	Colour	M.wt	M.P °C	Yield %	R_f	Element Analysis Found (calcul.) %. C	H	N	O	Found (calcul.) Metal %
ONMILA= $C_{19}H_{22}O_8N_2$	Deep brown	406.38	127	80.47	0.48	56.15 (55.93)	5.45 (5.31)	6.89 (6.94)	31.49 (31.7)	——
$[Co(L)Cl_2(H_2O)]H_2O$	Reddish-Brown	572.25	151	74.71	0.43	39.87 (39.49)	4.57 (4.59)	4.88 (4.67)	27.95 (27.81)	10.29 (9.74)
$[Ni(L)Cl_2(H_2O)]3H_2O$	Olive	608.04	145	70.13	0.41	37.53 (37.46)	4.97 (4.9)	4.6 (4.72)	31.57 (31.74)	9.65 (9.05)
$[Cu(L)Cl_2(H_2O)]H_2O$	Deep green	576.86	187	82.36	0.37	39.55 (39.71)	4.54 (4.42)	4.85 (4.54)	27.73 (27.9)	11.01 (11.24)
$[Zn(L)Cl(H_2O)_2]Cl.3H_2O$	ale brown	632.74	191 °D	73.2	0.40	36.06 (35.45)	5.09 (5.23)	4.42 (4.69)	29.43 (29.49)	10.33 (10.17)
$[Cd(L)Cl(H_2O)_2]Cl.2H_2O$	Deep beige	661.76	173 °D	65.68	0.35	34.48 (33.9)	4.56 (4.47)	4.23 (4.29)	29.01 (29.25)	16.98 (16.42)

3.2 N.M.R Spectra for the ONMILA Ligand

1H-NMR spectrum in Figure 1 (500 MHz in DMSO-d6) showed numerous signals. A carboxylic-OH low signal strength was seen at δ 11.85 ppm (s, 1H). The Pyridine ring showed multiplet signals at δ 7.7-7.21 (m, 3H) (Lee & McCarthy, 2019). A doublet peak at δ 5.25, δ 5.22 (d, 1H) was due to CH-4 lactone ring. The signals at δ 4.84, δ 4.73 (m, 2H) were assigned to CH-5, and the signals at δ 3.79 (s, 2H) and δ 3.71 (t, 2H) were attributed to pyridine-CH2 and CH2-6 l-ascorbic acid moieties, while that at δ 2.73 (s, 3H), 2.45 (s, 3H) were due to CH3- pyridine and CH3-N of 2-aminomethyl moieties. A single peak at δ 1.51 (s, 6H) ppm was attributed to (CH3)2 of 5,6-O-iso propylidene (Al-Noor et al., 2021).

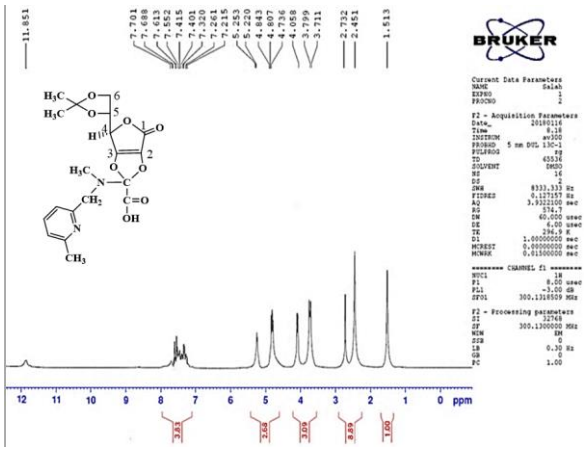

Figure 1. 1H-NMR spectrum of ONMILA.

DOI:https//doi.org/10.22452/mjs.vol42no3.7
Malaysian Journal of Science 42(3): 45-55 (October 2023)

There was a carboxylic acid peak at 176.04 ppm in the 13C-NMR spectrum as shown in Figure 2, with lactones ring carbon and pyridine (C=N) signal also present. Carbons (C-2 and C-3) were responsible for the two peaks at (137.22 and 142.71) ppm. There is a possibility that the "double bond that was conjugated from (C-1 to C-3)" shifted the (C-3) signal upfield (Lee & McCarthy, 2019) while the signals in the range of (136,26-120.6) "ppm were dispensed to C=C" pyridine ring carbon atoms. The signals at (66.03) due to C10-N of 2-methylpyridine, and the peak at (55.95) were assigned to C9-N amino-methyl moieties, while the signals in the range of (73.6-66.03) ppm were assigned to (C5-C4) and (C5-C-6). C-C carbon atoms C-7 and C-8 were responsible for the signals at 33.81, 29.23, and 27.13 ppm respectively (Lee & McCarthy, 2019; Al-Noor et al., 2021).

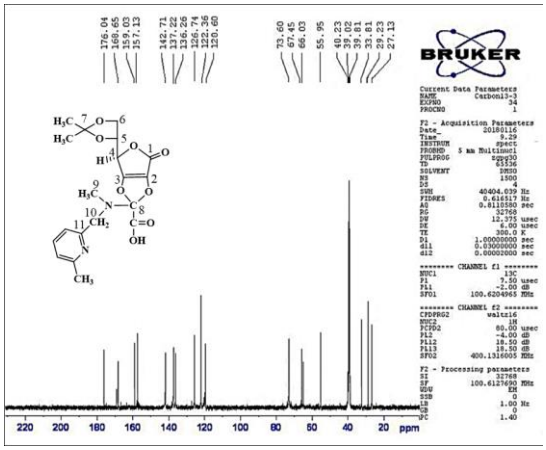

Figure 2. 13C-NMR spectrum of ONMILA.

3.3 Mass Spectrum for ONMILA

It was discovered that the molecular ion top at (m/z+ =406.2) in the ligand's mass spectrum as described in Figure 3 corresponded with (C19H22N2O8) (Ahmed et al., 2015; Gao, (2021). Scheme 2 summarises the pieces and their relative abundance.

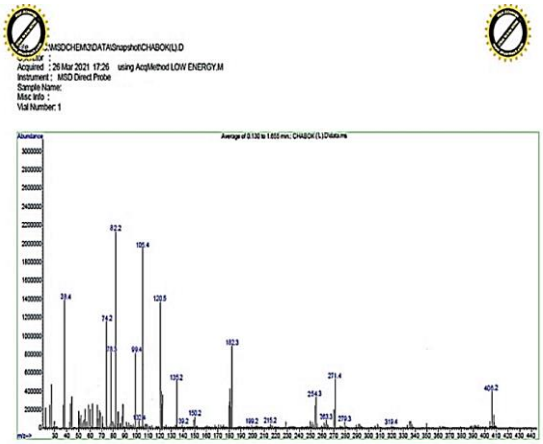

Figure 3. Mass spectrum of ONMILA.

DOI:https//doi.org/10.22452/mjs.vol42no3.7
Malaysian Journal of Science 42(3): 45-55 (October 2023)

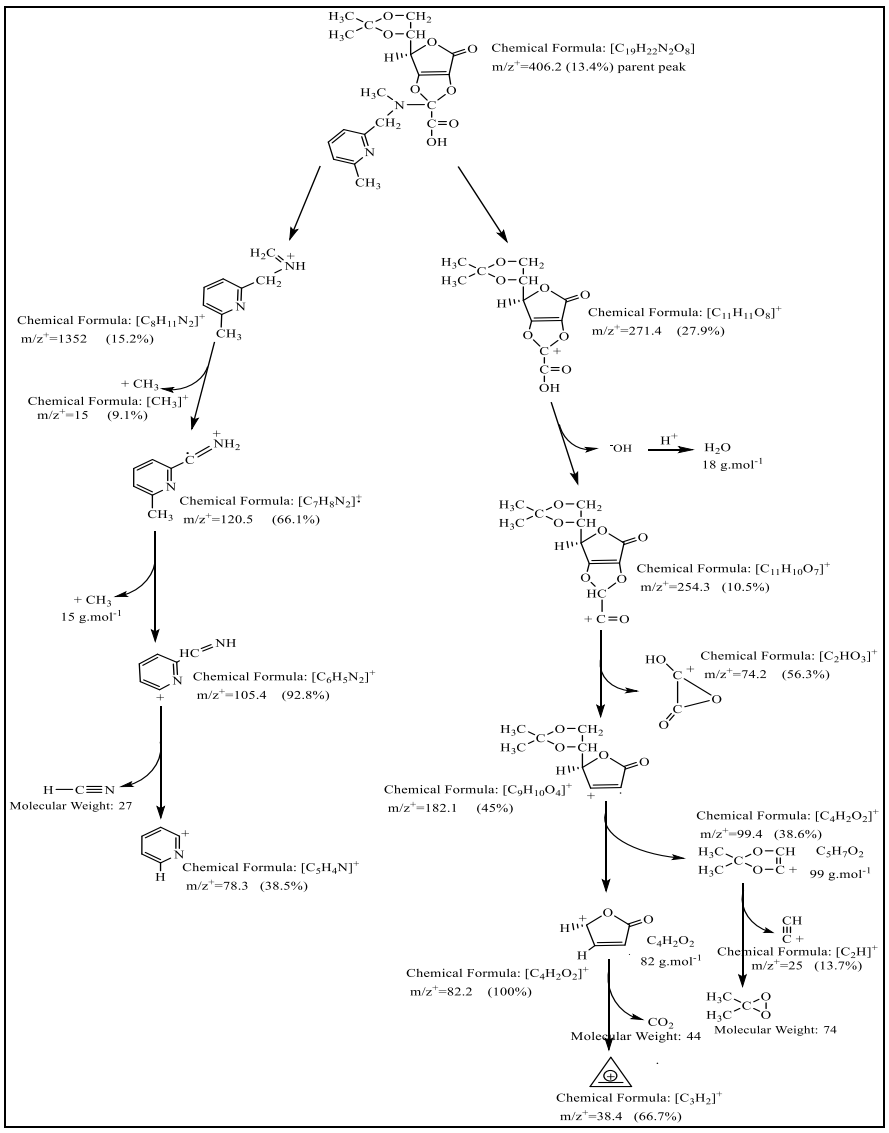

Scheme 2. The fragmentation of ONMILA.

3.4 Infrared Spectra of ONMILA and its Complexes

A comparison of ONMILA (FT-IR) spectrum and its metal complexes (nickel complex, for example) is shown in Figure 4 and Figure 5 . Table 2 summarises the major I.R. bands and their potential assignments. The frequency of the essential wide band at 3429 cm-1, which may be attributed to the OH-carboxylic acid in the free ligand, did not change for any complexes in the range of 3435-3416 cm-1 (Waddai et al., 2015). A band that was produced at (1627) cm-1 and was ascribed to the (C=N) stretching vibration of pyridine-N was linked with u(C=C) altered in shape and moved to a lower frequency in all complexes in the range of (1611-1595) cm-1 (El-Sonbati et al., 2016; Naji, 2014). Broad bands at (3419, 3435, 3416, 3432, and 3422) cm^{-1} due to (O-H) stretching in conjunction with OH-carboxyl stretching and bands at (807, 861, 855, 869, and 874) cm^{-1} in Co(II), Cu(II), Ni(II), Zn(II), and Cd(II) complexes respectively attributable to coordination water were found in all complexes (Waddai et al., 2015; Al-Farhan et al., 2021). The stretching vibration to the (C=O) ring of lactones was found at (1710) cm^{-1}, with a slight frequency shift in the range (1695-1723) cm^{-1} due to it not being involved in the coordination (Waddai et al., 2015; Radisavljević & Petrović, 2020). The stretching band (C=O)-carboxyl was found at (1685) cm^{-1} with a shape change and lower frequency in the range (1668-1653) cm^{-1} caused by a complex framework with the metal ions (Lawal et al., 2017). New weak bands displayed in all metal complexes spectra in the low-frequency range at (518-483) cm^{-1} and (477-446) cm^{-1}) proved to bond (Kareem et al.; Raman & Sobha, 2010).

DOI:https//doi.org/10.22452/mjs.vol42no3.7
Malaysian Journal of Science 42(3): 45-55 (October 2023)

Table 2. Characteristics of FT-IR absorption bands of ONMILA and its complexes.

Empirical formula	υOH Carbox., Hydrat.	υC=O lactone	υC=O Carbox.	υC=N υC=C	υC-N pyridine	δH_2O aqua	υM-N	υM-O
(L) ONMILA	3429,b	1710,m	1685,sh	1627,s	1155,m	-	-	-
[Co(L)Cl_2(H_2O)]H_2O	3419,b	1719,m	1653,s	1598,s	1118,m	807,w	518,w	454,w
[Ni(L)Cl_2(H_2O)]3H_2O	3435,b	1698,s	1668, m	1605,m	1125,w	861,w	483,w	446,w
[Cu(L)Cl_2(H_2O)]H_2O	3416,b	1714,m	1659,s	1611,s	1132,m	855,w	511,w	477,w
[Zn(L)Cl(H_2O)$_2$]Cl.3H_2O	3432,b	1723,s	1666,s	1609,m	1121,w	869,w	487,w	461,w
[Cd(L)Cl(H_2O)$_2$]Cl.2H_2O	3422,b	1695,s	1660,m	1605,m	1129,m	874,w	501,w	470,w

s= sharp, m= medium, w= weak, b= broad, sh=shoulder

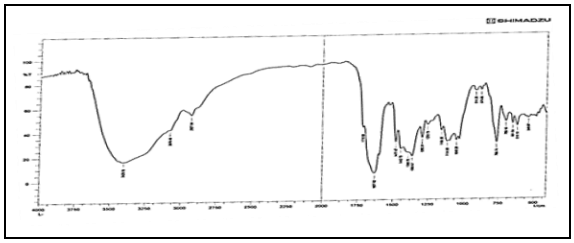

Figure 4. FT-IR spectrum of ONMILA.

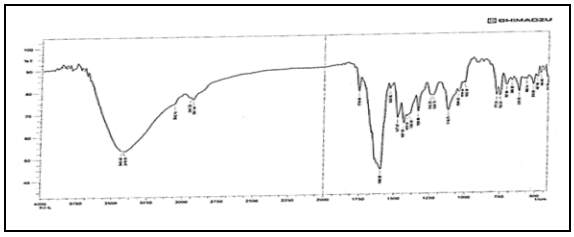

Figure 5. FT-IR spectrum of Ni(II) complex with ONMILA.

3.5 Electronic spectra

Table 3 lists the electronic absorption bands. Uv-Visible spectrum of ONMILA revealed three absorptions as shown in Figure 6 - two at (261 nm, 38341 cm^{-1}) and the other at (334 nm, 29940 cm^{-1}) due to the π–π^*, and one at (411 nm, 24330 cm^{-1}) attributable to the n–π^* transition (Ahmed et al., 2015). Two bands that emerged at 825 nm, 12121 cm^{-1} in Figure 7 electronic spectra for the Co-complex in ethanol solution were ascribed to the $^4T_1g \rightarrow {}^4A_2g$ (υ_2) and $^4T_1g \rightarrow {}^4T_1g_{(p)}$ (υ_3) transitions of octahedral geometry (Ahmed et al., 2015). Using the diagram of Tanaba-Sugano for the d^7 arrangement of octahedral geometry, the $B_{complex}$ (607.14) value as well as the position of υ_1 (9621 cm^{-1}) were computed using the ratio of (υ_3)/(υ_2) (1.35). (Nisah et al., 2021). The covalent nature is shown by the value of β (0.62). Three bands can be seen in the visible part of the Ni(II) complex's spectrum at (425 nm, 23512 cm^{-1}) $^3A_2g \rightarrow {}^3T_1g_{(P)}$ (υ_3), (702 nm, 14226cm^{-1}) $^3A_2g \rightarrow {}^3T_1g_{(F)}$ (υ_2), the final one at (9183 cm^{-1}) $^3A_2g \rightarrow {}^3T_2g_{(F)}$, ($\upsilon_1$). On the Tanaba-Sugano diagram, the ratio of υ_2/υ_1 1.54, was used for the d^8 octahedral complexes (Ahmed et al., 2016), $B_{complex}$ (694.7), and β (0.67). Broadband at (760 nm, 13157 cm^{-1}) in the Cu(II) complex spectrum was due to the $^2Eg \rightarrow {}^2T_2g$ transition, which is related to the Jahn-Teller distortion of the octahedral geometry (O'Toole et al., 2019). There was no visible bands in the Cd(II) and Zn(II) complexes spectra as described in Figures 8, 9; instead, there were only bands associated with charge transfer transitions (348 nm, 28735 cm^{-1}) Zn(II) (321 nm, 31152 cm^{-1}) When contrasted were free ligand, there was a presence of two bands at (237 nm, 42194 cm^{-1}) and at (263 nm, 38022 cm^{-1}) (Mutlu et al., 2020).

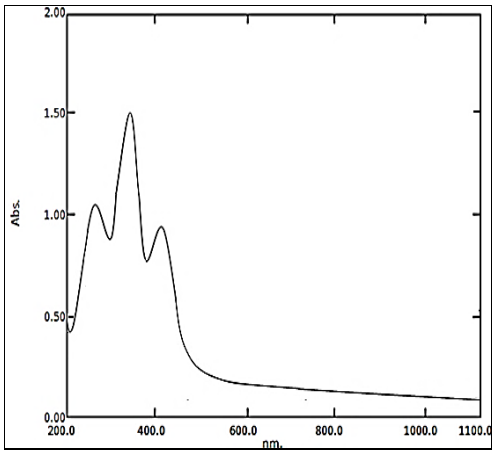

Figure 6. Electronic spectrum of ONMILA.

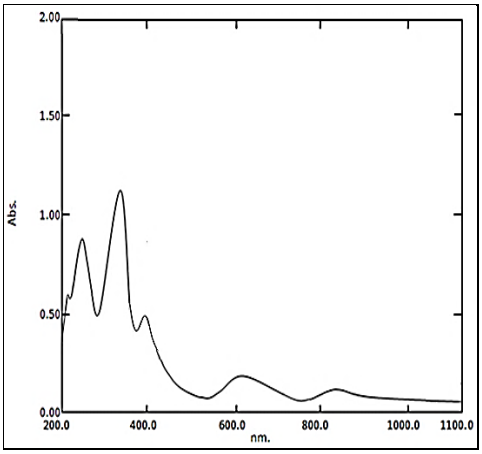

Figure 7. Electronic spectrum of ONMILA-Co(II) complex.

DOI:https//doi.org/10.22452/mjs.vol42no3.7
Malaysian Journal of Science 42(3): 45-55 (October 2023)

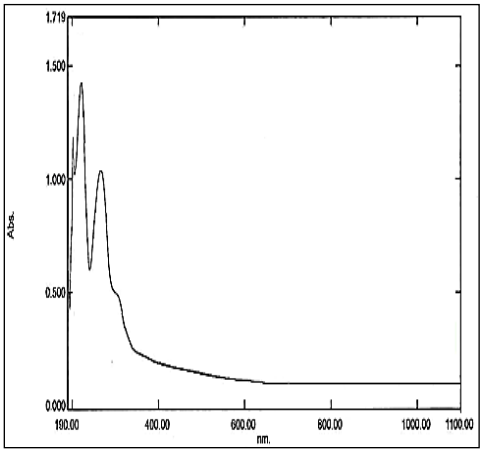

Figure 8. Electronic spectrum of ONMILA-Zn(II) Complex

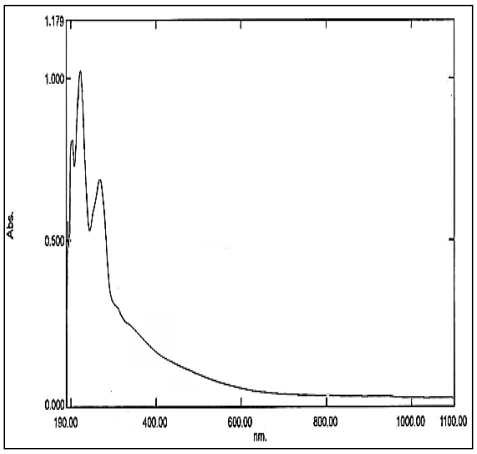

Figure 9. Electronic spectrum of ONMILA-Cd(II) Zn(II) complex.

3.6 Magnetic measurements

The magnetic moment's values possessed by the complexes were used in order to ascertain the coordination of the metal ion. Due to the inherent orbital angular momentum, there is always a big orbital contribution in the ground state, and the effective magnetic moment at ambient temperature was between (4.7 and 5.2 B.M.). The magnetic moment magnitude of the present complex, which was 4.83 B.M., suggested that the Co(II) complex in its high-spin form has the structure of an octahedron (Ahmed et al., 2016). The orbital contribution magnitude is what determines the greater range of values of magnetic moment (2.9-3.4 B.M.) for the complex of a high-spin Ni(II). The magnetic moment obtained in this investigation, 3.16, was in the expected range like octahedral Ni(II) ions (Ahmed et al., 2016). The Cu(II) complex magnetic moment was 1.76 B.M., and it was rather near to the spin value expected for one unpaired electron at 1.73 B.M.. As a result, the Cu(II) complex has the structure of an octahedron (Mutlu et al., 2020; Padmaningrum et al., 2022). According to Sanchez-Lara et al., 2021, the diamagnetic magnetic moments values of the metal complexes Zn(II) and Cd(II) are equal to those of the (d^{10}) configuration. Table 3 lists the magnetic moments that have been measured.

3.7 Conductivity measurements

All soluble complexes were dissolved in ethanol solvent ($1x10^{-3}$ M) at room temperature and they showed molar conductivity values of (38.07 – 12.95) $S.cm^2.mol^{-1}$". The complexes of Co(II), Cu(II) and Ni(II) had low conductivity and a non-ionic structure (Ahmed et al., 2016) while the conductivity tests of Cd(II) and Zn(II) revealed them as electrolytes (Yoe & Jones, 1944). Table 3 shows the conductivity values.

Table 3. Electronic spectra of ONMILA and its metal complexes, measurements of Racah parameter B', nephelauxetic parameter β, magnetic and conductivity values.

Compound	Band position nm	Band position cm^{-1}	Assignments	B' cm^{-1}	β	Λ.M $S.cm^2.mol^{-1}$	μ_{eff} B.M	Proposed Structure
ONMILA (L)	261 334 411	38341 29940 24330	$\pi\rightarrow\pi^*$ $n\rightarrow\pi^*$	— —	— —	———	——	———
L-Co(II)	610 825	16393 12121	$^4T_1g\rightarrow{}^4T_1g(p)$ $^4T_1g\rightarrow{}^4A_2g$	607.14	0.62	15.31	4.83	Octahedral Sp^3d^2
L-Ni(II)	425 702 1088	23512 14226 9183	$^3A_2g\rightarrow{}^3T_1g(p)$ $^3A_2g\rightarrow{}^3T_1g(F)$ $^3A_2g\rightarrow{}^3T_2g(F)$	694.7	0.67	12.95	3.16	Octahedral Sp^3d^2
L-Cu(II)	760	13157	$^2Eg\rightarrow{}^2T_2g$	—	—	16.02	1.76	Octahedral Sp^3d^2
L-Zn(II)	348	28735	M-L.C.T	—	—	37.84	Dia.	Octahedral Sp^3d^2
L-Cd(II)	321	31152	M-L C.T	—	—	39.07	Dia.	Octahedral Sp^3d^2

C.T. = Ligand Field Charge Transfer

DOI:https//doi.org/10.22452/mjs.vol42no3.7
Malaysian Journal of Science 42(3): 45-55 (October 2023)

3.8 Proposed Molecular Structures of Prepared Complexes

Earlier studies (Ahmed *et al*., 2016; Mutlu *et al*., 2020; Nisah *et al*., 2021; Padmaningrum *et al*., 2022) have examined the coordination sites available in the ligand and how they are related to various metal ions. The spectroscopic and analytical results based on the molar ratio, elemental analysis metal contents, magnetic measurements and the molar electrical conductivity measurements, as well as the results of the ^{1}H-NMR spectrum, the ^{13}C-NMR spectrum, the UV-Vis spectra and the infrared (FT-IR) spectra all indicated the complexes had octahedral geometry where the ligand behaved as tridentate coordination process. The oxygen of the carbonyl group and two nitrogen atoms of the 6-methyl-2-pyridylmethyl amine bound the ligand to metal ions in addition to water as aqua and chloro ion resulting in six donated atoms to the metal ions, Figures (10 and 11) describe the geometrical aspects of these compounds. There is a 1:1 mole ratio of M to L in these structures.

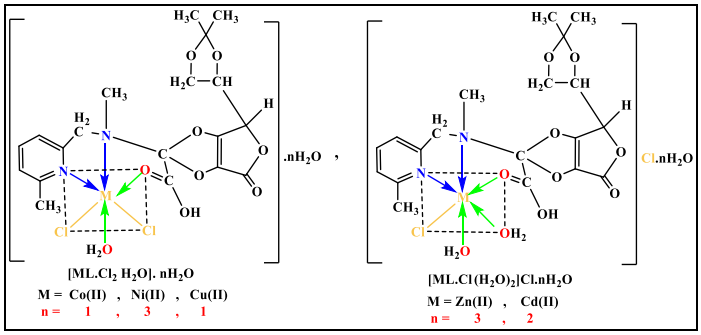

Figure 10. The suggested structure of metals ion complexes with ONMILA.

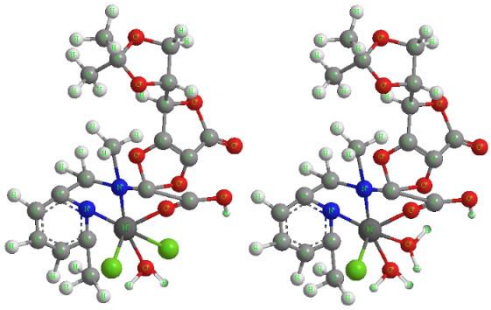

Figure 11. The proposed molecular 3D structure of ONMILA complexes.

3.9 Biological activity

The *in-vitro* growth inhibitory ligand activities and their complexes on Gram (+) bacteria, such as *Staphylococcus aureus* and *Streptococcus pyogenes* and Gram (-) bacteria, namely *Klebsiella pneumonia* and *E-coli*, were investigated using the spotted diffusion method. All of the substances exhibited a significant level of antibacterial activity when tested against the organisms in question. The *Streptococcus pyogenes* and *Staphylococcus aureus* were sensitive to the ligand and its complexes indicating that the biological activity of the complexes ranged from moderate to high. The Cd(II) complex showed higher antibacterial activity, either *E. coli* or *K. pneumonia*. There was only a slight amount of activity with the ligand and the complexes of Co(II), Cu(II) and Ni(II) while Cu(II) and Zn(II) showed moderate activity. However, the Cd(II) complex showed higher antibacterial activity from either *E. coli* or *K. pneumonia.* The cause of this resistance is the bacteria that live in the colon. These bacteria exist as a single bacillus and have a thick shell that completely encases their cell. The high lipid content of this coating helps to prevent them from entering the cell, in contrast to the bacteria *Staphylococcus aureus* and *Streptococcus pyogenes* which lack this characteristic. They will have a reduced ability to withstand the effects of chemical and antibiotic chemicals that penetrate the inside of the bacterial cell (Shiekhzadeh *et al*., 2020; Abu-Dief *et al*., 2020). As a direct consequence of this, the chemical agents that were investigated had a more powerful inhibiting effect. Since the metal ions included inside metal complexes were lipophilic, metal complexes have a higher activity level than free ligands (Omotade *et al*., 2020). There is also the possibility that these complexes contain antibacterial capabilities which would stop the multiplication of microbes by blocking the active sites of the organisms (Xue *et al*., 2020). The impermeability of the microorganisms' cells or alterations in the ribosomes of the microbial cells determine the effectiveness of different complexes against the germs that have been tested (Abdel-Rahman *et al*., 2016). According to Overtone's theory and chelation as described by Tweedy (1964), the metal ion polarity is significantly decreased during the chelation process because of overlaps of the ligand orbital and the slight sharing of the metal ion positive with donor groups. Additionally, the –electron delocalisation is magnified throughout the chelate sphere resulting in an increase in the lipophilicity of the complex. Through the process of chelation, the core metal atom becomes more lipophilic, which makes it possible for it to traverse the lipid layer of the cell membrane (Pang *et al*., 2019). Variations in the antibacterial activity are caused by the properties of metal ions as well as the cell membranes of the microorganisms. According to (Hameed *et al*., 2021), cell wall function inhibition, cell membrane and nucleic acid generation are the four different modes of action that may be attributed to antibacterial medications. These data are presented in Table 4, and the graphical representation of the statistics may be seen in Figure 12.

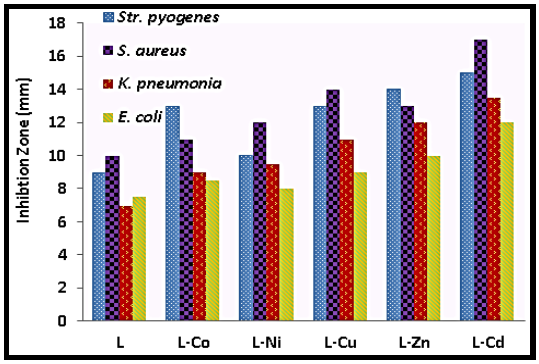

Figure 12. Statistical representation of antibacterial activity for ONMILA and its complexes.

DOI:https//doi.org/10.22452/mjs.vol42no3.7
Malaysian Journal of Science 42(3): 45-55 (October 2023)

Table 4. Inhibition area (mm) of the bacterial sensitivity (zone inhibition) to the compounds.

Compound	Pathogenic Bacteria			
	Str. pyogenes G(+)	*S. aureus* G(+)	*K. pneumonia* G(-)	*E. coli* G(-)
Ligand (L)	++	++	+	+
$[Co(L)Cl_2(H_2O)]H_2O$	+++	++	+	+
$[Ni(L)Cl_2(H_2O)]3H_2O$	++	+++	+	+
$[Cu(L)Cl_2(H_2O)]H_2O$	+++	+++	++	+
$[Zn(L)Cl(H_2O)_2]Cl.3H_2O$	++	+++	++	++
$[Cd(L)Cl(H_2O)_2]Cl.2H_2O$	+++	+++	+++	++

Not: (6-9) mm = + (A bit active), (9-12) mm= ++ (Moderate active),

(12-17) mm= +++ (High level of activity)

4. Conclusion

Spectroscopic analyses, such as elemental analysis, metal content, mass spectrum, 1H,13C-NMR, I.R., and UV-Vis, were used in this research to examine metal ions complexes of the new ligand. Conductivity measurements and magnetic susceptibility testing supported the octahedral geometry of all complexes. There was a 1:1 mole ratio of M to L in these structures. The biological activity of each chemical pointed to its antibacterial properties.

5. Acknowledgement

The author expresses his gratitude to the staff of Department of Chemistry, Faculty of Science, Kufa University for their support which resulted in the completion of this research paper. A big thank you is also due to Dr Lekaa Khalid and lecture Duha Mohammed for their research assistance.

6. References

Abdel-Rahman L H., Abu-Dief A M., Ismael M., Mohamed M A., Hashem N A. (2016). Synthesis, structure elucidation, biological screening, molecular modeling and DNA binding of some Cu (II) chelates incorporating imines derived from amino acids, *Journal of Molecular Structure, 1103*: 232-244.

Abu Dief A M, Abdel Rahman L H., Abdel Mawgoud A H. (2020). A robust in vitro anticancer, antioxidant and antimicrobial agents based on new metal-azomethine chelates incorporating Ag (I), Pd (II) and VO (II) cations: Probing the aspects of DNA interaction, *Applied Organometallic Chemistry, 34, no. 2*, *e5373*: 1-20.

Ahmed A. H., Hassan A. H., Gumaa A. B., Mohamed H., Eraky A M. (2016). Nickel (II)-oxaloyldihydrazone complexes: Characterization, indirect band gap energy and antimicrobial evaluation, *Cogent Chemistry, 2, no. 1*: *1142820*: 1-14.

Ahmed N., Riaz M., Ahmed A., Bhagat M. (2015). Synthesis, characterisation, and biological evaluation of Zn (II) complex with tridentate (NNO Donor) schiff base ligand, *International Journal of Inorganic Chemistry, 2015*: 1-5.

Al-Farhan B S., Basha M T., Abdel Rahman L H., El-Saghier A M., El-Ezz D A., Marzouk A., Shehata M R., Abdalla E. M. (2021). Synthesis, DFT Calculations, Antiproliferative, Bactericidal Activity and Molecular Docking of Novel Mixed-Ligand Salen/8-Hydroxyquinoline Metal Complexes, *Molecules, 26, no. 16*: 4725.

Al-Khafagy A. (2016). Synthesis, characterization and biological study of some new metal-azo chelate complexes, *Journal of Chemical and Pharmaceutical Research, 8, no. 8*: 296-302.

Al-Noor T H., Mohapatra R K., Azam M., AbdulKarem L K., Mohapatra P K., Ibrahim A A., Parhi P K., Dash G C., El-ajaily M., Al-Resayes S I., Raval M K., Pintilie L. (2021). Mixed-ligand complexes of ampicillin derived Schiff base ligand and Nicotinamide: Synthesis, physico-chemical studies, DFT calculation, antibacterial study and molecular docking analysis, *Journal of Molecular Structure, 1229*: 129832.

Bellavite P., Donzelli A. (2020). Hesperidin and SARS-CoV-2: New Light on the Healthy Function of Citrus Fruits, *Antioxidants, 9, 742*: 1-18.

Chatterjee I. (1973). "Evolution and the biosynthesis of ascorbic acid, *Science, 182, no. 4118*: 1271-1272.

El-Sonbati A., El-Bindary A., Mohamed G., Morgan S M., Hassan W., Elkholy A. (2016). Geometrical structures, thermal properties and antimicrobial activity studies of azodye complexes, *Journal of Molecular Liquids, 218*: 16-34.

DOI:https//doi.org/10.22452/mjs.vol42no3.7
Malaysian Journal of Science 42(3): 45-55 (October 2023)

Fodor G., Arnold R., Mohacsi T., Karle I., Flippen-Anderson J. (1983). A new role for L-ascorbic acid: Michael donor to α, β-unsaturated carbonyl compounds, *Tetrahedron, 39, no. 13*: 2137-2145.

Gao K., Mi H. (2021). Application of Membrane-Inlet Mass Spectrometry to Measurements of Photosynthetic Processes, *Research Methods of Environmental Physiology in Aquatic Sciences, Springer:* 187–192.

Hameed G F., Wadday F Y., Farhan M A A., Hussain S A. (2021). Synthesis, Spectroscopic characterization and bactericidal valuation of some metal (II) complexes with new Tridentate Heterocyclic Azo Ligand Type (NNO) Donor, *Egyptian Journal of Chemistry,64, no.3*:10-11.

Hanukoglu I. (2006). Antioxidant protective mechanisms against reactive oxygen species (ROS) generated by mitochondrial P450 systems in steroidogenic cells, *Drug metabolism reviews,38, no. 1-2*: 171-196.

Hariprasath K., Deepthi B., Babu I., Venkatesh S P., Sharfudeen S., Soumya V. (2010). Metal complexes in drug research-a review, *Journal of Chemical and Pharmaceutical Research, 2, no. 4*: 496-499.

Hollis L S., Amundsen A R., Stern E W. (1985). Synthesis, structure and antitumor properties of platinum complexes of vitamin C, *Journal of the American Chemical Society, 107, no. 1*: 274-276.

John N., James C. (2009). Scientific opinion of the panel on food additive and nutrient sources added to food on a request from the commission on calcium ascorbate, magnesium ascorbate and zinc ascorbate added for nutritional purposes in food supplements, *The European Food Safety Authority Journal, 994*: 1-22.

Kareem M J., Al-Hamdani A A., Al Zoubi Y K., Mohammed S G. (2021). Synthesis, characterization, and determination antioxidant activities for new Schiff base complexes derived from 2-(1H-indol-3-yl)-ethylamine and metal ion complexes, *Journal of molecular Structure, 1231*, *129669*: 1-18.

Lawal M., Obaleye J A., Bamigboye M. O., Nnabuike G G., Ayinla S O., Rajee, A O., Babamale H. F., Ajibola A A. (2017). Mixed metal complexes of isoniazid and ascorbic acid: chelation, characterization and antimicrobial activities, *Nigerian Journal of Chemical Research, 22, no. 1*: 20-28.

Loke W M., Proudfoot J M., McKinley A J., Croft K D. (2006). Augmentation of monocyte intracellular ascorbate in vitro protects cells from oxidative damage and inflammatory responses, *Biochemical and biophysical research communications, 345, no. 3*: 1039-1043.

Mutlu Gençkal H., Erkisa M., Alper P., Sahin S., Ulukaya E., Ari F. (2020). Mixed ligand complexes of Co (II), Ni (II) and Cu (II) with quercetin and diimine ligands: Synthesis, characterization, anti-cancer and anti-oxidant activity, *JBIC Journal of Biological Inorganic Chemistry, 25, no. 1*: 161-177.

Naji S H. (2014). Synthesis, Spectroscopic and biological studies of some metal complexes with 2,4–dinitro–2'–amino hydrazo benzene Al- Mustansiriyah *Journal of Science, 25, No.2*: 73-88.

Nisah K., Ramli M., Idroes R., Safitri E. (2021). Study of linearity and stability of Pb (II)-1, 10-phenanthroline complex with the presence of Fe (II) dan Mg (II) matrix ions using UV-Vis spectrophotometry, in *IOP Conference Series: Materials Science and Engineering*, *1087, 012052*, *no. 1*: *IOP Publishing*: 1-7.

O'Toole N., Lecourt C., Suffren Y., Hauser A., Khrouz L., Jeanneau E., Brioude A., Luneau D, Desroches C. (2019). Photogeneration of manganese (III) from luminescent manganese (II) complexes with thiacalixarene ligands: Synthesis, structures and photophysical properties, *European Journal of Inorganic Chemistry, 2019, no. 1*: 73-78.

Omotade E., Oviawe A., Elemike E. (2020). Synthesis, Characterization And Antimicrobial Activity Of Mixed Ligand Complexes of Benzyliminothiosemicarbazide And L-Phenylalanine With Divalent Fe, Co and Ni, *Journal of Chemical Society of Nigeria, 45, no. 2*: 282 - 289.

Padayatty S J., Katz A., Wang Y., Eck P., Kwon O., Lee J., Chen S., Corpe C., Dutta A., Dutta S K., Levine M. (2003). Vitamin C as an antioxidant: evaluation of its role in disease prevention, *Journal of the American college of Nutrition, 22, no. 1*: 18-35.

Padmaningrum R. T., Louise I S Y., Yunita I., Sugiyarto K H. (2022). Infrared Spectral And Magnetic Properties Of Basic Copper(Ii) Nitrate Produced By Slow Titration Method, *Malaysian Journal Of Science, 41(1)*: 106-116.

Pang Z., Raudonis R., Glick B R., Lin T J., Cheng Z. (2019). Antibiotic resistance in Pseudomonas aeruginosa: mechanisms and alternative therapeutic strategies, *Biotechnology advances, 37, no. 1*: 177-192.

Radisavljević S., Petrović B. (2020). Gold (III) complexes: An overview on their kinetics, interactions with DNA/BSA, cytotoxic activity, and computational calculations, *Frontiers in chemistry, 8, 379*: 1-8.

Raman N., Sobha S. (2010). Synthesis, characterization, DNA interaction and antimicrobial screening of isatin-based polypyridyl mixed ligand Cu (II) and Zn (II) complexes, *Journal of the Serbian Chemical Society, 75, no. 6*: 773-788.

DOI:https//doi.org/10.22452/mjs.vol42no3.7
Malaysian Journal of Science 42(3): 45-55 (October 2023)

Sánchez-Lara E., García-García A., González-Vergara E., Cepeda J., Rodríguez-Diéguez A. (2021). Magneto-structural correlations of cyclo-tetravanadates functionalized with mixed-ligand copper (ii) complexes, *New Journal of Chemistry, 45, no. 11*: 5081-5092.

Shiekhzadeh A., Sohrabi N., Moghadam M E., Oftadeh M. (2020). Kinetic and thermodynamic investigation of human serum albumin interaction with anticancer glycine derivative of platinum complex by using spectroscopic methods and molecular docking, *Applied Biochemistry and Biotechnology, 190, no. 2*: 506-528.

Tweedy B. (1964). Plant extracts with metal ions as potential antimicrobial agents, *Phytopathology, 55*: 910-914.

Valarmathy G., Subbalakshmi R., Sumathi R., Renganathan R. (2020). Synthesis of Schiff base ligand from N-substituted benzenesulfonamide and its complexes: Spectral, thermal, electrochemical behavior, fluorescence quenching, in vitro-biological and in-vitro cytotoxic studies, *Journal of Molecular Structure, 1199*: 127029.

Waddai F Y., Musa F H., Fidhel H A. (2015). Synthesis And Characterization Of Some Metal Complexes With Bis [O, O-2, 3; O, O-5, 6-(N, N-Dicarboxylic Methylidene)-N-2-Methylenepyridyl]-L-Ascorbic Acid, *European Chemical Bulletin*, *4, no. 2*: 74-79.

Wasi N., Singh H., Gajanana A., Raichowdhary A. (1987). Synthesis of metal complexes of antimalarial drugs and in vitro evaluation of their activity against plasmodium falciparum, *Inorganica chimica acta, 135, no. 2*: 133-137.

Xue L W., Zhang H J., Wang P P. (2020). Synthesis, crystal structures, and antimicrobial activity of copper(II) complexes derived from N'-(1-(pyridin-2-yl)ethylidene)isonicotinohydrazide, *Inorganic and Nano-Metal Chemistry, 50, no. 8*: 637-643.

Yoe J. H., Jones A L. (1944). Colorimetric determination of iron with disodium-1, 2-dihydroxybenzene-3, 5-disulfonate, *Industrial and Engineering Chemistry Analytical Edition, 16, no. 2*: 111-115.

Zümreoglu-Karan B. (2006). The coordination chemistry of Vitamin C: An overview, *Coordination Chemistry Reviews, 250, no. 17-18*: 2295-2307.

DOI:https//doi.org/10.22452/mjs.vol42no3.7
Malaysian Journal of Science 42(3): 45-55 (October 2023)